Gas-Phase Identity S_N2 Reactions of Halide Anions and Methyl Halides with Retention of Configuration

Mikhail N. Glukhovtsev,*[,1a,b] Addy Pross,*[,1a,c] H. Bernhard Schlegel,*[,1d] Robert D. Bach,[1e] and Leo Radom*[,1f]

Contribution from the School of Chemistry, University of Sydney, Sydney, NSW 2006, Australia, Department of Chemistry, Ben Gurion University of the Negev, Beer Sheva, Israel, Department of Chemistry, Wayne State University, Detroit, Michigan 48202, Department of Chemistry, University of Delaware, Newark, Delaware 19716, and Research School of Chemistry, Australian National University, Canberra, ACT 0200, Australia

Received June 17, 1996[⊗]

Abstract: High-level ab initio molecular orbital calculations at the G2(+) level of theory have been carried out on the identity front-side nucleophilic substitution reactions with retention of configuration, $X^- + CH_3X$, for X = F, Cl, Br, and I. Overall gas-phase barrier heights do not show a strong variation with halogen atom and are calculated to be 184.5 (X = F), 193.8 (X = Cl), 178.9 (X = Br), and 171.4 kJ mol^{-1} (X = I), substantially higher than the corresponding barriers for back-side attack (−8.0 for X = F, 11.5 for X = Cl, 5.8 for X = Br, and 6.5 kJ mol^{-1} for X = I). The difference between the overall barrier for back-side attack and front-side attack is smallest for X = I (164.9 kJ mol^{-1}). Central barrier heights for front-side attack decrease in the following order: 241.0 (X = F), 237.8 (X = Cl), 220.0 (X = Br), and 207.4 kJ mol^{-1} (X = I). The minimum energy pathways for both back-side and front-side S_N2 reactions are found to involve the same ion−molecule complex ($X^-\cdots H_3CX$), with the front-side pathway becoming feasible at higher energies. Indeed, our results suggest that the chloride exchange in CH_3Cl, which has been found in gas-phase experiments at high energies, may be the first example of a front-side S_N2 reaction with retention of configuration at saturated carbon. Analysis of our computational data in terms of frontier orbital theory suggests that elongation of the bond between the central atom and X could be a significant factor in decreasing the unfavorable nature of the front-side S_N2 reaction with retention of configuration in going from X = F to X = I. Ion−molecule complexes $CH_3-X\cdots X^-$, which may be pre-reaction complexes in direct collinear halophilic attack, were found for X = Br and I but not for X = F and Cl. The calculated complexation energies (ΔH_{comp}) for halophilic complexes are considerably smaller (7.3 and 19.4 kJ mol^{-1} for X = Br and I, respectively) than those for the corresponding pre-reaction complexes for S_N2 attack at carbon (41.1 and 36.0 kJ mol^{-1} for X = Br and I, respectively). Nucleophilic substitution reactions at the halogen atom in CH_3X (X = F−I) (halophilic reactions) are highly endothermic and appear to represent an unlikely mechanistic pathway for identity halide exchange.

Introduction

Bimolecular nucleophilic substitution (S_N2) at saturated carbon holds a central role within organic chemistry, and consequently the stereochemistry of the reaction has been intensively investigated, both experimentally[2−7] and theoretically.[2,8−12] Both experimental and theoretical[8−12] studies show that the preferred stereochemical route in the gas phase is one of back-side attack with inversion of configuration, as opposed to front-side attack with retention of configuration, precisely as is observed in solution. While retention of configuration has been found in nucleophilic substitution reactions at saturated silicon,[13] early reports on the possibility of retention at saturated carbon[6] were not confirmed by further experiments.[7]

Recently, experimental data on the gas-phase identity S_N2 reaction of methyl chloride with chloride anion at higher energies have been interpreted by Bierbaum et al.[14] as evidence for a chloride exchange mechanism that differs from the traditional back-side S_N2 pathway. These authors suggested that Cl^- attacks CH_3Cl at the Cl atom, resulting in the formation of a $[CH_3\cdots Cl_2]^-$ complex in which the chlorine atoms have become equivalent. The breakup of this complex to regenerate reactants then opens up a pathway for chloride exchange:

$$^{37}Cl^- + CH_3{}^{35}Cl \rightarrow [CH_3\cdots Cl_2]^- \rightarrow {}^{35}Cl^- + CH_3{}^{37}Cl \quad (1)$$

This pathway, while it does involve front-side attack on CH_3-Cl, should be distinguished from front-side attack at carbon since

[⊗] Abstract published in *Advance ACS Abstracts,* October 15, 1996.

(1) (a) University of Sydney. (b) On leave from the Institute of Physical and Organic Chemistry, Rostov University, 194/3 Stachka Ave., Rostov on Don, 344104, Russian Federation. Current address: Department of Chemistry, Wayne State University, Detroit, MI 48202. (c) Ben-Gurion University of the Negev. (d) Wayne State University. (e) University of Delaware. (f) Australian National University.

(2) Comprehensive collections of both experimental and computational data up to 1991 may be found in the monographs: (a) Shaik, S. S.; Schlegel, H. B.; Wolfe, S. *Theoretical Aspects of Physical Organic Chemistry, The S_N2 Mechanism*; Wiley: New York, 1992. (b) Minkin, V. I.; Simkin, B. Y.; Minyaev, R. M. *Quantum Chemistry of Organic Compounds—Mechanisms of Reactions*; Springer Verlag: Berlin, 1990.

(3) Riveros, J. M.; Jose, S. M.; Takashima, K. *Adv. Phys. Org. Chem.* **1985**, *21*, 197.

(4) Lieder, C. A.; Brauman, J. I. *J. Am. Chem. Soc.* **1974**, *96*, 4028.

(5) Speranza, M.; Angelini, G. *J. Am. Chem. Soc.* **1980**, *102*, 3115.

(6) ElGomati, T.; Lenoir, D.; Ugi, I. *Angew. Chem., Int. Ed. Engl.* **1975**, *14*, 59.

(7) (a) Maryanoff, C. A.; Ogura, F.; Mislow, K. *Tetrahedron Lett.* **1975**, 4095. (b) Vergnani, T.; Karpf, M.; Hoesch, L.; Dreiding, A. S. *Helv. Chim. Acta* **1975**, *58*, 273.

(8) Stohrer, W.-D.; Schmieder, K. R. *Chem. Ber.* **1976**, *109*, 285.

(9) Schlegel, H. B.; Mislow, K.; Bernardi, F.; Bottoni, A. *Theor. Chim. Acta* **1977**, *44*, 245.

(10) Anh, N. T.; Minot, C. *J. Am. Chem. Soc.* **1980**, *102*, 103.

(11) Minot, C. *Nouv. J. Chim.* **1981**, *5*, 319.

(12) Basilevsky, M. V.; Koldobskii, S. G.; Tikhomirov, V. A. *Russian Chem. Rev.* (*Engl. Transl.*) **1986**, *55*, 948.

(13) Corriu, R. J. P.; Guerin, C. *J. Organomet. Chem.* **1980**, *198*, 231.

(14) Barlow, S. E.; Van Doren, J. M.; Bierbaum, V. M. *J. Am. Chem. Soc.* **1988**, *110*, 7240.

S0002-7863(96)02019-7 CCC: $12.00

the initial attack is presumed to take place at halogen, a so-called halophilic reaction,[15] rather than at carbon. Evidence for gas-phase nucleophilic attack on halogen has been presented by Cyr et al.,[16] who found that at high collision energies Cl^- attacks the halogen in CH_3Br in a halogen abstraction reaction:

$$CH_3Br + Cl^- \rightarrow CH_3^{\bullet} + Br{-}Cl^{\bullet -} \qquad (2)$$

While the study by Bierbaum et al.[14] does suggest that the gas-phase halogen exchange at high energies proceeds by some pathway other than back-side S_N2, its precise nature must be considered still unresolved. The question arises: does front-side nucleophilic attack take place at the halogen atom, or does it take place at the carbon atom?

In order to resolve this issue, we have undertaken a high-level computational study of the potential energy surface for front-side attack of methyl halides with halide anions for the set of identity S_N2 reactions:

$$CH_3X + {}^*X^- \rightarrow CH_3{}^*X + X^- \qquad (X = F, Cl, Br, and I) \qquad (3)$$

and of the corresponding halophilic reactions:

$$CH_3X + X^- \rightarrow [CH_3XX^-]^{\ddagger} \rightarrow CH_3^{\bullet} + XX^{\bullet -} \qquad (X = F, Cl, Br, and I) \quad (4)$$

$$CH_3X + X^- \rightarrow [CH_3XX^-]^{\ddagger} \rightarrow CH_3^- + XX \qquad (X = F, Cl, Br, and I) \quad (5)$$

Our aim is to define the various possible reaction pathways that would be classified within the general category of front-side attack, to calculate the energetics of these reaction pathways, and to assess their relative feasibility, as well as their feasibility in comparison with the more conventional back-side S_N2 reaction.

Computational Methods

It is clear from the very large number of calculations already carried out on S_N2 reactions at carbon[2,12,18−23] that the computational data are very sensitive to the level of theory employed. For this reason, in our earlier study of identity S_N2 halide-exchange with inversion of configuration at carbon,[23] we used a level of theory, specifically a modification[23] of G2 theory,[24] that describes the energetics at a higher level than has been used in previous comparative studies.[2,8−12,20, 21a,22] At this level of theory, the results appeared to agree with available experimental data and suggested that meaningful barrier heights can be obtained computationally.[23] In the present study, we apply this same level of theory to the set of reactions with retention of configuration.

Standard ab initio molecular orbital calculations[25] were carried out using a modified form[23] of G2 theory[24] with the GAUSSIAN 92 system of programs.[26] G2 theory corresponds effectively to calculations at the QCISD(T)/6-311+G(3df,2p) level with zero-point vibrational energy (ZPE) and higher level corrections. It has been shown[24,27] to perform well for the calculation of atomization energies, ionization energies, electron affinities, bond energies, proton affinities, acidities, and reaction barriers.

For a better description of anions, we have used the G2(+) modification[23] of G2 theory. Geometries were optimized and vibrational frequencies determined with a basis set that includes diffuse functions, specifically 6-31+G(d) in place of 6-31G(d) for first- and second-row atoms. In addition, the MP2/6-31+G(d) optimizations were carried out with the frozen-core approximation rather than with all electrons being included in the correlation treatment as in standard G2 theory. We have recently extended G2(+) calculations to bromine- and iodine-containing species[28] utilizing the effective core potentials (ECP) developed by Hay and Wadt,[30] and such calculations were performed for the Br- and I-containing species in the present study.

Geometries were optimized using analytic gradient techniques.[31] The eigenvalue-following method[32] was employed in the search for transition structures in the halophilic reactions. The algorithm developed by Schlegel and Gonzalez[33] was used for following the intrinsic reaction coordinate downhill from the transition structure for front-side attack. Stationary points on the potential energy surfaces were characterized

(15) (a) Zefirov, N. S.; Makhon'kov, D. I. *Chem. Rev.* **1982**, *82*, 615. (b) For nucleophilic substitution at bromine, see: Beak, P.; Allen, D. J. *J. Am. Chem. Soc.* **1992**, *114*, 3420.

(16) Cyr, D. M.; Scarton, M. G.; Wiberg, K.; Johnson, M. A.; Nonose, S.; Hirokawa, J.; Tanaka, H.; Kondow, T.; Morris, R. A.; Viggiano, A. A. *J. Am. Chem. Soc.* **1995**, *117*, 1828.

(17) Cyr, D. M.; Bishea, G. A.; Scarton, M. G.; Johnson, M. A. *J. Chem. Phys.* **1992**, *97*, 5911.

(18) Cernusak, I.; Urban, M. *Collect. Czech. Chem. Commun.* **1988**, *53*, 2239.

(19) (a) Shi, Z.; Boyd, R. J. *J. Am. Chem. Soc.* **1990**, *112*, 6789. (b) Shi, Z.; Boyd, R. J. *J. Am. Chem. Soc.* **1991**, *113*, 1072. (c) Boyd, R. J.; Kim, C-K.; Shi, Z.; Weinberg, N.; Wolfe, S. *J. Am. Chem. Soc.* **1993**, *115*, 10147.

(20) (a) Zhao, X. G.; Tucker, S. C.; Truhlar, D. G. *J. Am. Chem. Soc.* **1991**, *113*, 826. (b) Hu, W.-P.; Truhlar, D. G. *J. Am. Chem. Soc.* **1994**, *116*, 7797. (c) Wladkowski, B. D.; Allen, W. D.; Brauman, J. I. *J. Phys. Chem.* **1994**, *98*, 13532.

(21) Harder, S.; Streitwieser, A.; Petty, J. T.; Schleyer, P. v. R. *J. Am. Chem. Soc.* **1995**, *117*, 3253.

(22) Deng, L.; Branchadell, V.; Ziegler, T. *J. Am. Chem. Soc.* **1994**, *116*, 10645.

(23) Glukhovtsev, M. N.; Pross, A.; Radom, L. *J. Am. Chem. Soc.* **1995**, *117*, 2024.

(24) (a) Curtiss, L. A.; Raghavachari, K.; Trucks, G. W.; Pople, J. A. *J. Chem. Phys.* **1991**, *94*, 7221. For recent reviews on G2 theory, see: (b) Curtiss, L. A.; Raghavachari, K. In *Quantum Mechanical Electronic Structure Calculations with Chemical Accuracy*; Langhoff, S. R., Ed.; Kluwer: Dordrecht, 1995. (c) Raghavachari, K.; Curtiss, L. A. In *Modern Electronic Structure Theory*; Yarkony, D. R., Ed.; World Scientific: Singapore, 1995; p 991.

(25) Hehre, W. J.; Radom, L.; Schleyer, P. v. R.; Pople, J. A. *Ab Initio Molecular Orbital Theory;* Wiley: New York, 1986.

(26) Frisch, M. J.; Trucks, G. W.; Head-Gordon, M.; Gill, P. M. W.; Wong, M. W.; Foresman, J. B.; Johnson, B. G.; Schlegel, H. B.; Robb, M. A.; Replogle, E. S.; Gomperts, R.; Andres, J. L.; Raghavachari, K.; Binkley, J. S.; Gonzalez, C.; Martin, R. L.; Fox, D. J.; DeFrees, D. J.; Baker, J.; Stewart, J. J. P.; Pople, J. A. GAUSSIAN-92, Gaussian Inc.: Pittsburgh, PA, 1992.

(27) See, for example (a) Smith, B. J.; Radom, L. *J. Phys. Chem.* **1991**, 95, 10549. (b) Ma, N. L.; Smith, B. J.; Pople, J. A.; Radom, L. *J. Am. Chem. Soc.* **1991**, *113*, 7903. (c) Nobes, R. H.; Radom, L. *Chem. Phys. Lett.* **1992**, *189*, 554. (d) Yu, D.; Rauk, A.; Armstrong, D. A. *J. Phys. Chem.* **1992**, *96*, 6031. (e) Wong, M. W.; Radom, L. *J. Am. Chem. Soc.* **1993**, *115*, 1507. (f) Smith, B. J.; Radom, L. *J. Am. Chem. Soc.* **1993**, *115*, 4885. (g) Schlegel, H. B.; Skancke, A. *J. Am. Chem. Soc.* **1993**, *115*, 7465. (h) Goldberg, N.; Hrusák, J.; Iraqi, M.; Schwarz, H. *J. Phys. Chem.* **1993**, *97*, 10687. (i) Armstrong, D. A.; Rauk, A.; Yu, D. *J. Am. Chem. Soc.* **1993**, *115*, 666. (j) Wiberg, K.; Rablen, P. R. *J. Am. Chem. Soc.* **1993**, *115*, 9234. (k) Wiberg, K.; Nakaji, D. *J. Am. Chem. Soc.* **1993**, *115*, 10658. (l) Su, M.-D.; Schlegel, H. B. *J. Phys. Chem.* **1993**, *97*, 8732. (m) Darling, C. L.; Schlegel, H. B. *J. Phys. Chem.* **1993**, *97*, 1368. (n) Su, M.-D.; Schlegel, H. B. *J. Phys. Chem.* **1993**, *97*, 9981. (o) Lammertsma, K.; Prasad, B. V. *J. Am. Chem. Soc.* **1994**, *116*, 642. (p) Gauld, J. W.; Radom, L. *J. Phys. Chem.* **1994**, *98*, 777. (q) Chiu, S.-W.; Li, W.-K.; Tzeng, W.-B.; Ng, C.-Y. *J. Chem. Phys.* **1992**, *97*, 6557. (r) Durant, J. L.; Rohlfing, C. M. *J. Chem. Phys.* **1993**, *98*, 8031. (s) Glukhovtsev, M. N.; Pross, A.; Radom, L. *J. Am. Chem. Soc.* **1994**, *116*, 5961. (t) Glukhovtsev, M. N.; Pross, A.; Radom, L. *J. Am. Chem. Soc.* **1995**, *117*, 9012.

(28) (a) Glukhovtsev, M. N.; McGrath, M. P.; Pross, A.; Radom, L. *J. Chem. Phys.* **1995**, *103*, 1878. (b) Note that we have recommended[28a] alternative ECP basis sets for bromine and iodine for use in *standard G2-(ECP)* calculations.[29]

(29) (a) Glukhovtsev, M. N.; Szulejko, J. E.; McMahon, T. B.; Gauld, J. G.; Scott, A. P.; Smith, B. J.; Pross, A.; Radom, L. *J. Phys. Chem.* **1994**, *98*, 13099. (b) Glukhovtsev, M. N.; Pross, A.; Radom, L. *J. Phys. Chem.* **1996**, *100*, 3498.

(30) Wadt, W. R.; Hay, P. J. *J. Chem. Phys.* **1985**, *82*, 284.

(31) (a) Schlegel, H. B. *J. Comput. Chem.* **1982**, *3*, 214. (b) Schlegel, H. B. In *Modern Electronic Structure Theory*; Yarkony, D. R., Ed.; World Scientific: Singapore, 1995; p 459.

(32) (a) Simons, J.; Jørgensen, P.; Taylor, H.; Ozment, J. *J. Phys. Chem.* **1983**, *87*, 2745. (b) Taylor, H.; Simons, J. *J. Phys. Chem.* **1985**, *89*, 684. (c) Baker, J. *J. Comput. Chem.* **1986**, *7*, 385. For a recent review, see: (d) McKee, M. L.; Page, M. In *Reviews in Computational Cheimstry;* Lipkowitz, K. B., Boyd, D. B., Eds.; VCH: New York, 1993; Vol. 4, p 35.

(33) Gonzalez, C.; Schlegel, H. B. *J. Phys. Chem.* **1990**, *94*, 5523.

Table 1. Geometries of $H_3CX\cdots X^-$ (X = Br (**3c**) and I (**3d**)) Ion−Molecule Complexes Calculated at the MP2/6-31+G(d) Level and Natural Charges Calculated at the MP2/6-311+G(3df,2p)//MP2/6-31+G(d) Level[a,b]

complex	r(C−X_b)	r(X···X)	r(C−H)	∠X_bCH	q(X_a)	q(X_b)	q(C)	q(H)
$H_3CBr\cdots Br^-$	1.958	3.529	1.090	109.0	−0.968	0.082	−0.686	0.190
$H_3CI\cdots I^-$	2.159	3.675	1.090	109.0	−0.928	0.166	−0.820	0.194

[a] Bond lengths in Å, bond angles in deg. [b] G2(+) complexation energies of **3c** and **3d** are 7.3 and 19.4 kJ mol^{-1}, respectively.

by the calculation of vibrational frequencies, which was performed analytically for X = F and Cl and numerically in ECP calculations of species containing Br and I. Charge distributions were obtained from the wave functions calculated at the MP2/6-311+G(3df,2p) level on MP2/6-31+G(d) geometries, employing natural population analysis (NPA).[34]

Calculated total energies are presented in of the Supporting Information. Unless otherwise stated, we have used the results of G2(+)-all electron (AE) calculations for F- and Cl-containing molecules and G2-(+)-ECP calculations for Br- and I-containing molecules in our analysis. Throughout this paper, relative energies are presented as enthalpy changes (ΔH) at 0 K, bond lengths are in angstroms, and bond angles are in degrees. Of course at 0 K, relative enthalpies (ΔH) and relative energies (ΔE) are identical and the terms are used interchangeably here.

Results and Discussion

The reactions of CH_3X with X^- may be divided into two general types: (i) nucleophilic substitution pathways (S_N2) which involve X^- attack at carbon, and which result in halide exchange (eq 3), and (ii) halophilic reaction pathways which generally lead to dihalogen formation (eqs 4 and 5), but which have also been postulated as being able to lead to a halogen exchange reaction (eq 1). While the S_N2 reaction at carbon might, at least in principle, take place by either front- or back-side attack, the halophilic reaction, given that it involves nucleophilic attack at halogen, would by definition be a front-side pathway.

The potential energy surface for a gas-phase reaction between an ion and a neutral molecule is generally expected to show the initial formation of an ion−molecule complex.[35,36] Thus the minimum energy pathway involving back-side nucleophilic attack at carbon (leading to an S_N2 reaction with inversion of configuration) is typically found to proceed through a loose C_{3v} ion−molecule complex **1** followed by a D_{3h} transition structure **2**.[2,12] Let us now consider possible structures for complexes on the reaction pathways associated with front-side attack.

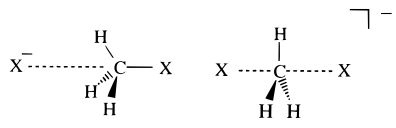

1 (C_{3v}) **2** (D_{3h})

(**a**: X = F; **b**: X = Cl; **c**: X = Br; **d**: X = I)

A. Ion−Molecule Complexes and Transition Structures for the S_N2 Reaction with Retention of Configuration. Two possible additional candidates for ion−molecule intermediates for front-side attack at carbon in CH_3X (leading to an S_N2 reaction with retention of configuration) are the C_{3v} complex **3**, in which the incoming nucleophile coordinates with the halogen atom, and the C_s structure **4**, in which the nucleophile is also coordinated to one of the methyl hydrogens.[8,9] While all our attempts to locate minima for structures of type **4** were unsuccessful, we did find minima corresponding to complexes **3** for X = Br and I, though not for X = F or Cl.[37] The absence of minima corresponding to the complex **3** for X = F or Cl may be explained by the fact that the fluorine and chlorine atoms in methyl halides are found to bear negative charges (NPA charges at the MP2/6-311+G(3df,2p) level are −0.400 and −0.063, respectively).[23] In contrast, the bromine and iodine atoms in the CH_3X bear positive charges of 0.016 and 0.121, respectively.[38]

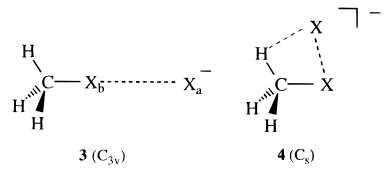

3 (C_{3v}) **4** (C_s)

(**a**: X = F; **b**: X = Cl; **c**: X = Br; **d**: X = I)

The two front-side coordinate complexes that were located, **3c** and **3d**, are quite weakly bound in comparison with the corresponding back-side complexes, **1c** and **1d**. Thus, the complexation energy for $H_3C-Br\cdots Br^-$ (**3c**) is only 7.3 kJ mol^{-1} compared with a value of 41.1 kJ mol^{-1} for $Br^-\cdots H_3C-Br$ (**1c**).[23] Similarly, the complexation energies for the corresponding iodine-containing species, **3d** and **1d,** are 19.4 and 36.0 kJ mol^{-1}, respectively,[23] the former value being close to results of earlier calculations by Hu and Truhlar.[37] Given the significant drop in complexation energies on proceeding from $H_3C-I\cdots I^-$ to $H_3C-Br\cdots Br^-$, it is not surprising that the analogous complexes, $H_3C-F\cdots F^-$ (**3a**) and $H_3C-Cl\cdots Cl^-$ (**3b**) were not found. The X···X distances in the complexes **3c** and **3d** (3.529 and 3.675 Å, respectively, see Table 1) are shorter than the contact distances for van der Waals interaction and the upper limits for specific interactions (3.79 and 4.13 Å, respectively).[39] However, these X···X distances are longer than those in the $X_2^{\bullet-}$ radical anions (Table 2). The C−Br and C−I

(34) (a) Reed, A. R.; Weinstock, R. B.; Weinhold, F. *J. Chem. Phys.* **1985**, *83*, 735. (b) Reed, A. E.; Curtiss, L. A.; Weinhold, F. *Chem. Rev.* **1988**, *88*, 899. (c) Weinhold, F.; Carpenter, J. E. In *The Structure of Small Molecules and Ions*; Naaman, R., Vager, Z., Eds.; Plenum Press: New York, 1988; p 227. (d) Reed, A. E.; Weinhold, F. *Isr. J. Chem.* **1991**, *31*, 277. For recent NPA applications, see, e.g.: (e) Reed, A. E.; Schleyer, P. v. R. *J. Am. Chem. Soc.* **1990**, *112*, 1434. (f) Glukhovtsev, M. N.; Schleyer, P. v. R. *Chem. Phys. Lett.* **1992**, *198*, 547. (g) Mestres, J.; Duran, M.; Bertran, J. *Theor. Chim. Acta* **1994**, *88*, 325. (h) Nemukhin, A. V.; Grigorenko, B. L. *Chem. Phys. Lett.* **1995**, *233*, 627.

(35) (a) Olmstead, W. N.; Brauman, J. I. *J. Am. Chem. Soc.* **1977**, *99*, 4219. (b) Pellerite, M. J.; Brauman, J. I. *J. Am. Chem. Soc.* **1980**, *102*, 5993. (c) Pellerite, M. J.; Brauman, J. I. *J. Am. Chem. Soc.* **1983**, *105*, 2672. (d) Pellerite, M. J.; Brauman, J. I. In *Mechanistic Aspects of Inorganic Reactions*; Rorabacher, D. R., Endicott, J. F., Eds.; ACS Symposium Series; American Chemical Society: Washington, DC, 1982; Vol. 198, p 81. (e) Barfknecht, A. T.; Dodd, J. A.; Salomon, K. E.; Tumas, W.; Brauman, J. I. *Pure Appl. Chem.* **1984**, *56*, 1809.

(36) Dedieu, A.; Veillard, A. In *Quantum Theory of Chemical Reactions*; Daudel, R., Pullman, A., Salem, L., Veillard, A., Eds.; Reidel: Dordrecht, 1980, p 69.

(37) A previous search by Hu and Truhlar for minima corresponding to various complexes of methyl iodide and iodide anion also revealed just the two forms, **1d** and **3d**. For details, see: Hu, W.-P.; Truhlar, D. G. *J. Phys. Chem.* **1994**, *98*, 1049.

(38) We note, however, that a CHELPG analysis predicts a negative charge on I in CH_3I. See: Storer, J. W.; Giesen, D. J.; Cramer, C. J.; Truhlar, D. G. *J. Comput.-Aided Mol. Des.* **1995**, *9*, 87.

(39) (a) Zefirov, Yu. V.; Zorkii, P. M. *Russ. Chem. Rev.* (*Engl. Transl.*) **1989**, *58*, 421 . (b) Zefirov, Yu. V.; Porai-Koshits, M. A. *Zh. Strukt. Khim.* (*Engl. Transl.*) **1980**, *21*, 150. (c) Zefirov, Yu. V.; Porai-Koshits, M. A. *Zh. Strukt. Khim.* (*Engl. Transl.*) **1986**, *27*, 74. (d) VWRs were obtained from X-ray diffraction data on organic crystal structures (VWR(C) = 1.71 Å, VWR(F) = 1.40 Å, VWR(Cl) = 1.90 Å, VWR(Br) = 1.97 Å, VWR(I) = 2.14 Å). The expression $2(R_AR_B)^{1/2}$ is used to estimate interatomic distances for ordinary van der Waals interactions using VWRs of A and B atoms, respectively.[39a−c] The upper limit for specific interactions is approximated as $2(R_AR_B)^{1/2} - 0.15$ Å.[39c]

Table 2. Bond Lengths (Å) in X_2 (X = F, Cl, Br, and I) and $X_2^{\bullet-}$ Calculated at the MP2/6-31+G(d) Level as well as Corresponding Calculated G2(+) and Experimental Electron Affinities (EA, eV)

	r(X−X)[a]		EA(X_2)	
X	X_2	$X_2^{\bullet-}$	G2(+)	exptl[b]
F	1.434 (1.412)	1.916	3.01	2.9 ± 0.2
Cl	2.018 (1.988)	2.653	2.38	2.4 ± 0.2
Br	2.328 (2.281)	2.898	2.49	2.5 ± 0.1
I	2.685 (2.666)	3.253	2.37	2.5 ± 0.1[c]

[a] Experimental values, taken from ref 40, are given in parentheses. [b] Reference 41. [c] Other experimental values are 2.3, 2.4 ± 0.2, 2.4 ± 0.1, and 2.6 ± 0.1 eV, see ref 41.

bond lengths in **3c** and **3d** are elongated by 0.004 and 0.019 Å relative to those in CH_3Br and CH_3I, respectively.

While complexes **3c** and **3d** are possible candidates for the pre-reaction complexes for both front-side nucleophilic attack at carbon and for halophilic attack at halogen, at least for X = Br and I, the alternative possibility of a front-side attack pathway at high energies via **1** should also be considered. In order to determine which complex, **1** or **3**, actually serves as the entrance complex on the minimum energy pathway for front-side attack,[42] we have followed the reaction surface down from the front-side transition structure. Let us begin then by characterizing the transition structure for front-side attack.

Previous theoretical studies at the HF level of the reaction of F^- with CH_3F have shown that front-side attack proceeds via the C_s transition structure **5** with a perpendicular configuration of the X_2 moiety relative to one of the methyl C−H bonds:[9]

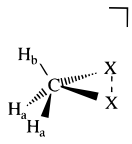

5 (C_s)

(**a**: X = F; **b**: X = Cl; **c**: X = Br; **d**: X = I)

In the present study, we also find the C_s structure **5** to be the transition structure for front-side attack (at the MP2/6-31+G(d) level). The important feature of transition structure **5** is that it contains equivalent halogen atoms. This is significant since it is this equivalence that provides a mechanism for halogen exchange. When we carry out symmetry-unconstrained geometry optimizations in search of minima starting from **5** (for X = F−I), we find that they all eventually lead to the "back-side" ion−molecule complex **1**, and not to the front-side complex **3** (for X = Br and I where they exist). In addition, we have followed the intrinsic reaction coordinate[33] downhill from **5** without any symmetry constraints at the HF/6-31+G(d) level and have observed the same results. This corroborates the results of recent DFT/LDA calculations[22] on the $Cl^- + CH_3Cl$ reaction, which indicated the intrinsic reaction path for a high-energy mechanism of reaction 1 for X = Cl to involve complex

Table 3. Geometries of $H_3CX_2^-$ (X = F−I) C_s Transition Structures (**5**) Calculated at the MP2/6-31+G(d) Level[a]

structure	r(C−X)	r(X···X)[b]	r(C−H_a)[c]	r(C−H_b)[c]	∠XCX	∠XCH_b
$H_3CF_2^-$	1.815	2.355	1.085	1.099	80.9	98.0
$H_3CCl_2^-$	2.438[d]	3.268	1.080	1.081	84.2[d]	94.1
$H_3CBr_2^-$	2.639	3.576	1.079	1.081	85.3	93.3
$H_3CI_2^-$	2.868	3.952	1.079	1.083	87.1	93.6

[a] Bond lengths in Å, bond angles in deg. The C_s structures **5a**−**d** have only one imaginary frequency at both the HF/6-31+G(d) and MP2/6-31+G(d) levels. [b] Upper limits for specific X···X interactions are 2.65 (F), 3.65 (Cl), 3.79 (Br), and 4.13 (I) Å. For details see refs 39a−c. [c] H_a and H_b atoms are as shown in **5**, see text.

Table 4. NPA Charge Distributions for the $CH_3X_2^-$ Transition Structures (**5**, X = F, Cl, Br, and I)[a]

species	q(C)	q(X)	q(H_a)	q(H_b)	q(CH_3)[b]
5a (X = F)	−0.082	−0.645	0.116	0.140	0.290
5b (X = Cl)	−0.320	−0.604	0.173	0.182	0.208
5c (X = Br)	−0.388	−0.576	0.178	0.184	0.152
5d (X = I)	−0.470	−0.531	0.175	0.182	0.062

[a] Calculated at the MP2/6-311+G(3df,2p) level. [b] The CH_3 group charge gives an estimate of the extent of the VB triple-ion $X^-R^+X^-$ configuration.[2a] For the D_{3h} transition structure **2** for back-side attack, the CH_3 group charges are larger: 0.432 (F); 0.254 (Cl); 0.188 (Br); 0.098 (I).[23]

1b. We have previously found[23] that optimizations starting from the transition structure **2** for backside attack of X^- on CH_3X also lead to the ion−molecule complex **1**. Thus, our results indicate that *the intrinsic reaction paths for both front-side and back-side S_N2 attack of X^- on CH_3X begin from the same pre-reaction ion−molecule complex **1***.

Before proceeding to discuss the nature of the reaction surface in detail, it is important to note that the implications of this result to the reaction dynamics are not straightforward. Thus the *actual* gas-phase reaction pathways do not necessarily follow every feature of the intrinsic reaction path. In particular, high-energy processes or reactions of high exothermicity may proceed without the involvement of a reaction intermediate, despite such an intermediate appearing on the minimum energy pathway. Also, in some cases the dynamic pathways may actually be quite different from the pathway described by the intrinsic reaction coordinate. Thus it is quite possible that high-energy front-side S_N2 reactions proceeding through transition structure **5** may not actually begin with the back-side complex *despite* the nature of the minimum energy pathway. With this proviso regarding the relationship of dynamic pathways and minimum energy pathways clarified, let us now discuss the details of the energy surface for both front-side and back-side pathways.

The energy profile for the front-side reaction is represented by a symmetric double-well potential (Figure 1), analogous to that for back-side attack (also illustrated in Figure 1),[3,35,36] though of substantially different energy. Initially, the reactants come together to form the pre-reaction ion−molecule complex, **1**, with a complexation energy, ΔH_{comp}. The ion−molecule complex must then overcome an activation barrier that we term the *central* barrier, $\Delta H^{\ddagger}_{cent}$, to reach transition structure **5**. The energy then drops with the formation of the product ion−molecule complex which finally dissociates into separated products. The *overall* activation barrier, i.e. the barrier relative to separated reactants, is denoted $\Delta H^{\ddagger}_{ovr}$.

Geometries and charge distributions for transition structures **5** are presented in Tables 3 and 4, respectively. While the X···X distances in **5** are longer than those in the $X_2^{\bullet-}$ radical anions or in the X_2 molecules (Table 2), they are shorter than the contact distance for van der Waals interactions as well as the upper limits for specific interactions,[39] suggesting some X--X bonding. The C−H bonds in **5** are all shortened relative to

(40) Huber, K. P.; Herzberg, G. *Molecular Spectra and Moleclar Structure. IV. Constants of Diatomic Molecules*; Van Nostrand Reinhold: New York, 1979.

(41) Lias, S. G.; Bartmess, J. E.; Liebman, J. F.; Holmes, J. L.; Levin, R. D.; Mallard, W. G. *J. Phys. Chem. Ref. Data* **1988**, *17*, Suppl. 1.

(42) A direct nucleophilic substitution mechanism initiated by exciting the C−X stretch mode, in which products are formed without the explicit involvement of either pre-reaction or post-reaction ion−molecule complex, may also be possible.[43] Studies of the reaction dynamics, for which our computational data on the PES would be useful, should consider this possibility.

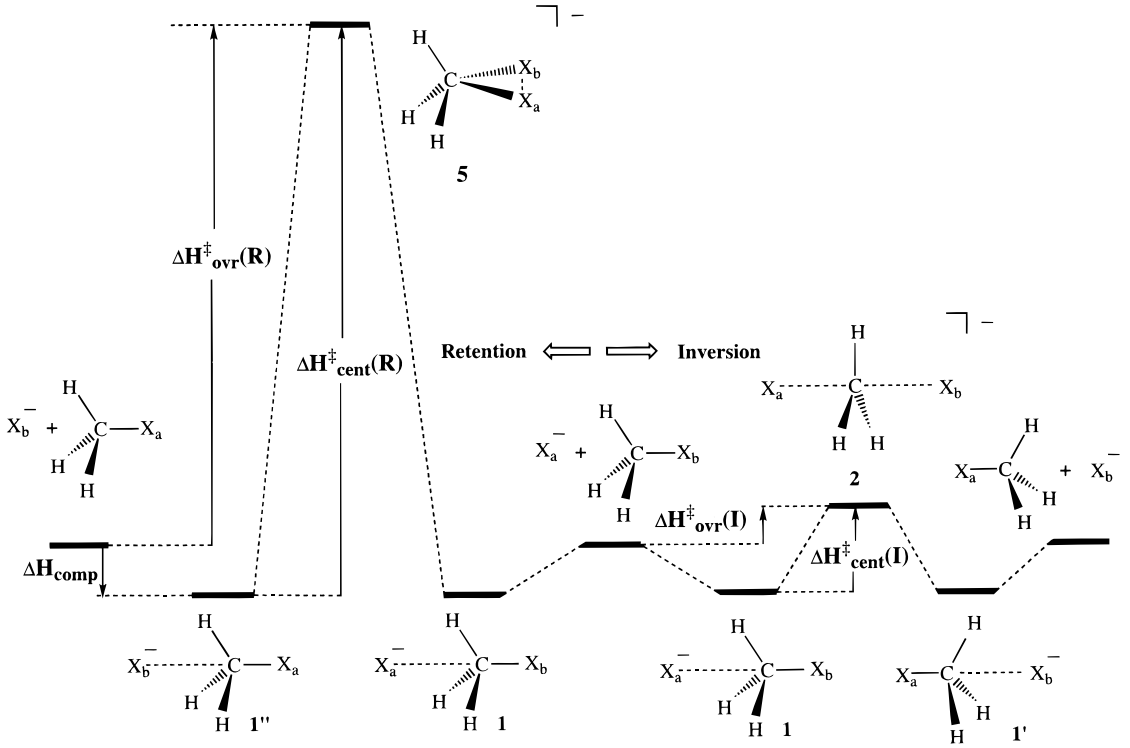

Figure 1. Schematic energy profile for the $X^- + CH_3X$ identity exchange reaction (X = F−I) with retention of configuration and with inversion of configuration.

those in CH_3X (Table 3). It is notable that although the C−X bond lengths in the C_s transition structures **5b**−**d** are longer than those in the D_{3h} transition structures **2b**−**d**,[23] the C−F bond length in **5a** is actually slightly shorter (by 0.022 Å) than that in **2a**.

The charge distributions within structures **2** and **5** allow the relative ionicities of the transition structures for the inversion and retention pathways to be compared. At the HF/6-31+G(d) level, the NPA charge on the CH_3 group in the C_s transition structure **5b** (0.725) was previously found[21] to be larger than that in **2b** (0.491). Also at the HF/6-31+G(d) level the C−Cl bond length in **5b** was found to be 0.397 Å longer than that in **2b**. These results led the authors to conclude that there is pronounced ionicity in the mechanism for front-side attack.[21] However, at the MP2/6-311+G(3df,2p) level, the CH_3 group NPA charges in **5a** (0.290) and **5b** (0.208) (Table 4) are considerably smaller than the values of 0.490 and 0.725 calculated at the HF/6-31+G(d) level.[21] Also, in general, the halogen atoms in **5** bear smaller negative NPA charges (Table 4) than in transition structure **2**.[23] Finally, we have found at the MP2/6-31+G(d) level that the C−Cl bond lengths in **5b** (2.438 Å) are quite close to those in **2b** (2.317 Å) (Table 3). Thus, the conclusion that the mechanism of the nucleophilic substitution reaction with retention of configuration is of a carbocation S_Ni type,[21] is not supported by our higher level data.

B. Barrier Heights for the S_N2 Reaction with Retention of Configuration. The barriers for front-side attack with retention of configuration, $\Delta H^{\ddagger}_{ovr}(R)$ and $\Delta H^{\ddagger}_{cent}(R)$, are given in Table 5. In all cases, the barriers are substantially greater than the corresponding values for back-side attack with inversion of configuration, $\Delta H^{\ddagger}_{ovr}(I)$ and $\Delta H^{\ddagger}_{cent}(I)$. However, the barriers for front-side attack are considerably smaller than C−X bond energies in the methyl halides,[23] indicating that the front-side pathway may well be followed at higher energies.

The variation in overall barrier height for front-side attack for different halogens is small but somewhat larger than for back-side attack. This results in the energy difference between the two reaction pathways decreasing somewhat, in going from

Table 5. Overall Barriers ($\Delta H^{\ddagger}_{ovr}$), and Central Barriers ($\Delta H^{\ddagger}_{cent}$) for Reactions 3 with Retention of Configuration (R) and with Inversion of Configuration (I) Calculated at the G2(+) Level (kJ mol^{-1})[a]

X	$\Delta H^{\ddagger}_{ovr}$(R)[b]	$\Delta H^{\ddagger}_{ovr}$(I)[b]	$\Delta H^{\ddagger}_{cent}$(R)[b]	$\Delta H^{\ddagger}_{cent}$(I)[b]
F	184.5	−8.0[c]	241.0[d]	48.5[c,e,f]
Cl	193.8[g]	11.5[c,h]	237.8[d]	55.5[c,e,i]
Br	178.9	5.8[c]	220.0	46.9[c]
I	171.4	6.5[c]	207.4	42.5[c]

[a] G2(+) overall barriers and central barriers for reaction 3 with inversion of configuration were taken from ref 23. [b] R and I stand for the reactions with retention and inversion of configuration, respectively. [c] LDA-SCF and NL-SCF calculations[22] underestimate the overall and central barriers for reaction 2 with inversion of configuration. All the overall barriers were found to be negative (−13.1 (F), −5.7 (Cl), −7.3 (Br), and −5.8 (I) kJ mol^{-1}) at the NL-SCF level.[22] The central barriers, $\Delta H^{\ddagger}_{cent}$(I), were calculated to be 28.4 (F), 19.2 (Cl), 13.0 (Br), and 7.5 (I) kJ mol^{-1} at the same level.[22] [d] The barrier heights, $\Delta H^{\ddagger}_{cent}$(R), found at the MP4/6-31+G(d)//HF/6-31+G(d) + ZPE(HF/6-31+G(d)) level[21] are 238.9 and 279.5 kJ mol^{-1} for X = F and Cl, respectively. [e] The barrier heights, $\Delta H^{\ddagger}_{cent}$(I), found at the MP4/6-31+G(d)//HF/6-31+G(d) + ZPE(HF/6-31+G(d)) level[21] are 41.0 and 65.3 kJ mol^{-1} for X = F and Cl, respectively. [f] The G2(+) central barrier for X = F (48.5 kJ mol^{-1}) may be compared with a barrier height of 53.6 ± 6.3 kJ mol^{-1} obtained by extrapolation from CCSD(T) calculations using a [13s8p6d4f,8s6p4d] basis set.[20c] [g] This value of the overall barrier (2.01 eV) agrees with the experimental estimate of the overall barrier for chloride exchange at higher energies (2.0 eV), see ref 14. [h] Experimental estimates are 4.2 ± 4.2 (ref 14) and 10.5 kJ mol^{-1} (ref 44a), respectively. The overall barrier determined by means of modeling the bimolecular kinetics with statistical phase space[44b] theory is 11.6 ± 1.0 kJ mol^{-1}. [i] Experimental estimate[14] is 55.2 ± 8.4 kJ mol^{-1}.

192.5 for X = F to 164.9 kJ mol^{-1} for X = I (Table 5, Figure 2). The central barriers for front-side attack appear to follow periodic ordering, decreasing from 241.0 (F) to 207.4 kJ mol^{-1} (I) (Table 5, Figure 3). Again the difference between the front-side and back-side barriers decreases from X = F to X = I.

It is of interest to examine our results in the light of predictions of earlier theoretical work. Frontier molecular orbital (FMO) theory[10−12,13,45] has been previously employed to rationalize the experimental and theoretical data on the stereochemistry of S_N2 reactions and, in particular, to predict

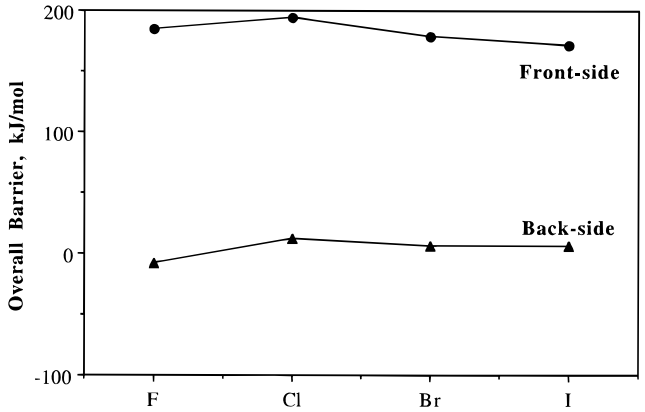

Figure 2. Trends in the G2(+) overall barriers of reaction 3 with retention of configuration ($\Delta H^{\ddagger}_{ovr}$(R)) and with inversion of configuration ($\Delta H^{\ddagger}_{ovr}$(I)) for the set of halogens. G2(+) $\Delta H^{\ddagger}_{ovr}$(R) and $\Delta H^{\ddagger}_{ovr}$(I) values are listed in Table 5.

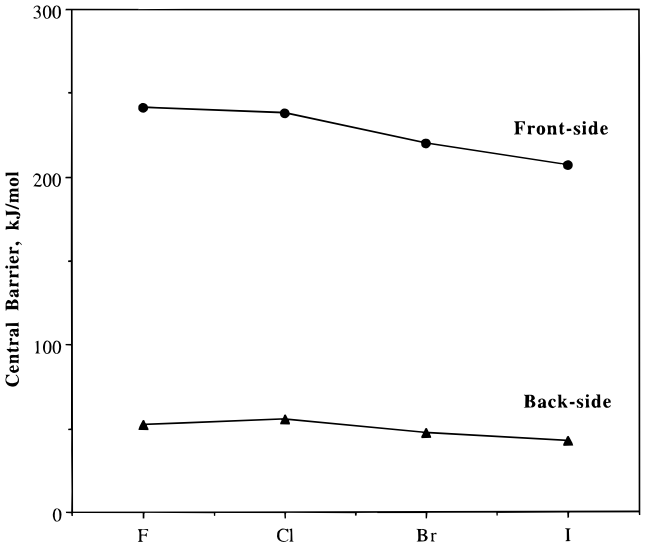

Figure 3. Trends in the G2(+) central barriers of reaction 3 with retention of configuration ($\Delta H^{\ddagger}_{cent}$(R)) and with inversion of configuration ($\Delta H^{\ddagger}_{cent}$(I)) for the set of halogens. G2(+) $\Delta H^{\ddagger}_{cent}$(R) and $\Delta H^{\ddagger}_{cent}$(I) values are listed in Table 5.

which factors are likely to favor retention of configuration. According to the FMO treatment, the major interaction during an S_N2 reaction is that between the highest occupied MO (HOMO) of the incoming nucleophile Nu^- and the lowest unoccupied MO (LUMO) of the substrate (Figure 4). The LUMO is mainly an out-of-phase combination (σ^*_{C-X}) of the carbon atomic φ_C orbital and the atomic φ_X orbital of the leaving atom.[10−12]

The FMO model suggests that switching the reaction stereochemistry from inversion of configuration to retention might be achieved if the in-phase overlap of the nucleophile HOMO and the φ_C orbital is increased, while the unfavorable overlap between the nucleophile HOMO and the atomic φ_X orbital is decreased (Figure 4). This led to the proposal[10,13] of four main factors that might favor the retention of configuration: (i) A leaving group X with a contracted atomic φ_X orbital would

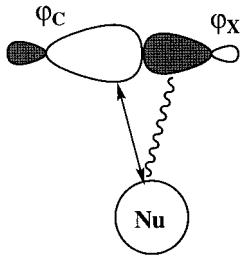

Figure 4. Schematic representation of interaction between the HOMO of the nucleophile and the σ^*_{C-X} orbital of the substrate during front-side nucleophilic attack. See text for details.

minimize the out-of-phase HOMO−φ_X overlap. Accordingly, the replacement of an element of larger atomic number by one of smaller atomic number within the same column of the periodic table (e.g. replacing X = Cl by X = F) would be predicted to favor the retention pathway. (ii) Employing a hard[46] nucleophile (e.g. F^- or RO^-) rather than a soft nucleophile (e.g. I^-) would also serve to reduce the out-of-phase HOMO−φ_X overlap. Here, also, retention would be predicted to be preferred for F^- over I^-. (iii) Decreasing the electronegativity of the central atom would increase the contribution of the φ_C orbital to the antibonding σ^*_{C-X} orbital, thereby leading to an increase in the favorable in-phase nucleophile HOMO−φ_C overlap. Thus, replacing carbon by silicon should make retention of configuration more feasible. (iv) Elongation of the bond between the central atom and X would favor retention because of a reduction in the unfavorable interaction between the incoming nucleophile and the leaving group. This last effect should favor X = Cl over X = F and operates in the opposite direction to effect (i). For nucleophilic attack at carbon, factors (i) and (ii) were taken to be larger than the opposing bond elongation effect (iv), leading to the general conclusion that retention of configuration would be relatively favored for the lighter elements within a column of the periodic table (i.e. retention would be relatively favored for X = F over X = I).[10]

While frontier-orbital theory is necessarily a simplified treatment whose limitations when applied to S_N2 reactions are well-documented,[47] the above predictions appear to be consistent with a large body of experimental data for nucleophilic substitution reactions at silicon (that proceed with both inversion and retention of configuration).[13,48−50] For substitution at carbon, however, our computational results suggest that the situation is more complicated. Our most striking finding is that the central and overall barriers for front-side S_N2 reaction for halide exchange vary within a relatively narrow range of just 33.6 and 22.4 kJ mol^{-1}, respectively (Table 5). Within the FMO framework described above, our result implies that the competition of factors (i)−(ii) vs factor (iv) leads to similar barrier heights. The fact that the energy difference between front-side and back-side attack barriers is actually the smallest for X = I (164.9 kJ mol^{-1} as compared with 192.5 kJ mol^{-1} for X = F) suggests that perhaps the bond length between the central atom and X might be the more important factor influencing the relative preference for front-side attack with retention of configuration over back-side attack with inversion of configuration in these systems.

(43) (a) Basilevsky, M. V.; Ryaboy, V. M. *Chem. Phys. Lett.* **1986**, *129*, 71. (b) Vande Linde, S. R.; Hase, W. L. *J. Chem. Phys.* **1990**, *93*, 7962. (c) Cho, Y. J.; Vande Linde, S. R.; Zhu, L.; Hase, W. L. *J. Chem. Phys.* **1992**, *96*, 8275. (d) Hase, W. L.; Cho, Y. J. *J. Chem. Phys.* **1993**, *98*, 8626.

(44) (a) Wladkowski, B. D.; Brauman, J. I. *J. Phys. Chem.* **1993**, *97*, 13158. (b) Graul, S. T.; Bowers, M. T. *J. Am. Chem. Soc.* **1994**, *116*, 3875.

(45) (a) Salem, L. *Chem. Br.* **1969**, *5*, 449. (b) Serre, J. *Int. J. Quantum Chem.* **1984**, *26*, 593. (c) Kato, H.; Morokuma, K.; Yonezawa, T.; Fukui, K. *Bull. Chem. Soc. Jpn.* **1965**, *38*, 1749.

(46) Pearson, R. G. In *The Concept of Chemical Bonding*; Maksic, Z. B., Ed.; Springer-Verlag: Berlin, 1990; p 45.

(47) (a) Bach, R. D.; Wolber, G. J. *J. Am. Chem. Soc.* **1984**, *106*, 1401. (b) Wladkowski, B. D.; Lim, K. F.; Allen, W. D.; Brauman, J. I. *J. Am. Chem. Soc.* **1992**, *114*, 9136.

(48) (a) Damrauer, R.; DePuy, C. H.; Bierbaum, V. M. *Organometallics* **1982**, *1*, 1553. (b) Damrauer, R.; Burggraf, L. W.; Davis, L. P.; Gordon, M. S. *J. Am. Chem. Soc.* **1988**, *110*, 6601. (c) Windus, T. L.; Gordon, M. S.; Davis, L. P.; Burggraf, L. W. *J. Am. Chem. Soc.* **1994**, *116*, 3568.

(49) (a) DePuy, C. H.; Damrauer, R.; Bowie, J. H.; Scheldon, J. C. *Acc. Chem. Res.* **1987**, *20*, 129. (b) Bowie, J. H. *Org. Mass Spectrom.* **1993**, *28*, 1407.

(50) Schlegel, H. B.; Skancke, P. N. *J. Am. Chem. Soc.* **1993**, *115*, 10916.

Table 6. G2(+) Calculated Enthalpies of Reactions 4 and 5 (kJ mol^{-1})

	$CH_3X + X^- \rightarrow$ dissociation products	
halogen X	$CH_3^\bullet + X_2^{\bullet-}$	$CH_3^- + X_2$
F	355.1	638.8
Cl	232.0	454.3
Br	189.2	422.7
I	158.2	379.5

Inclusion of the central atom into a small ring has been considered to preferentially favor front-side nucleophilic attack,[8,13] as predicted also by EHT calculations of reactions of cyclopropane derivatives.[51] Given our observation that the difference between the barrier heights for halide exchange with retention and with inversion of configuration is smallest for X = I (Table 5), our results suggest that reactions involving nucleophilic attack in small bridgehead iodides (which cannot undergo substitution via back-side attack) might be possible candidates for a front-side pathway. Solvolysis of 1,3-diiodobicyclo[1.1.1]pentane with methanol, which leads to 1-iodo-3-methoxybicyclo[1.1.1]pentane, is presumed to occur via the formation of a bridged cationic species.[52] It would, however, be of interest to examine the nucleophilic substitution of this and similar substrates under S_N2 conditions to test for the possibility of front-side attack with retention of configuration.

Our calculations allow an assessment of the likelihood of the possible halophilic pathways (eqs 4 and 5) in comparison with the two S_N2 pathways. Our results indicate that the energetics of the halophilic reactions are very unfavorable, all of them being highly endothermic (Table 6), with the products of reaction 4, $CH_3^\bullet + X_2^{\bullet-}$, lying lower in energy than those of reaction 5, $CH_3^- + X_2$ (Table 6).[53] In fact, given that the *products* of reactions 4 and 5 are actually higher in energy than the *transition structures* **5** for front-side nucleophilic attack at carbon in all but one case ($CH_3^\bullet + I_2^{\bullet-}$ is lower in energy than **5d** by 13.1 kJ mol^{-1}) (Table 5), we can conclude that both back-side and front-side nucleophilic attack at carbon in H_3CX (X = F−I) should generally be preferred over the halophilic pathways.

C. Mechanism of Chloride Exchange at Higher Energies. What light do our calculations throw on the mechanism of chloride exchange observed by Bierbaum et al.[14] at high energies? Given the large positive enthalpies (232.0 (eq 4b) and 454.3 kJ mol^{-1} (eq 5b), Table 6) for the halophilic reactions, and the fact that these energies for the products of halophilic attack, $CH_3^\bullet$ and $Cl_2^{\bullet-}$ and CH_3^- and Cl_2, are actually higher in energy than the transition structure **5b** for front-side S_N2 reaction (by 38.2 and 260.5 kJ mol^{-1}, respectively), the possibility of a halophilic reaction seems unlikely. A front-side S_N2 reaction would be both thermodynamically and kinetically preferred to the halophilic pathways 4b and 5b. Most significantly, our calculations predict an overall activation energy for front-side S_N2 attack on CH_3Cl by Cl^- of 193.8 kJ mol^{-1} (2.01 eV), in excellent agreement with the value reported by Bierbaum and co-workers for the high energy chloride exchange pathway (2.0 eV).[14] We conclude therefore that, in the gas-phase, halide exchange may occur by both back-side S_N2 reaction with inversion of configuration *and* front-side S_N2 reaction with retention of configuration, and that *the mechanism for chloride exchange for reaction 1 at saturated carbon found experimentally at higher energies*[14] *is likely to be the front-side S_N2 pathway.*

Conclusions

Application of G2(+) theory to front-side attack mechanisms in gas-phase identity S_N2 reactions of halide anions with methyl halides ($X^- + CH_3X$; X = F, Cl, Br, and I) leads to the following conclusions.

(1) Our calculations suggest that the Cl^- exchange in the reaction of $CH_3Cl + Cl^-$ that has been experimentally observed in the gas phase at high energies is the first example of an S_N2 reaction with retention of configuration at saturated carbon. The overall barrier for this reaction is calculated to be 193.8 kJ mol^{-1} (2.01 eV), in good agreement with the experimentally measured value of 2.0 eV.

(2) The intrinsic reaction paths for both back-side S_N2 with inversion of configuration and front-side S_N2 with retention of configuration involve the same C_{3v} ion−molecule complex, $X^-\cdots H_3CX$ **1**, though the barrier for the front-side reaction is significantly higher. Overall barriers for $X^- + CH_3X$ reactions with retention of configuration decrease from 193.8 (for X = Cl) to 171.4 kJ mol^{-1} (for X = I). The smallest difference between the overall barriers for the reaction with retention of configuration compared with those with inversion of configuration is found for X = I, but the difference remains substantial (164.9 kJ mol^{-1}).

(3) Central barrier heights ($\Delta H^{\ddagger}_{cent}$) for front-side attack of X^- at saturated carbon in CH_3X decrease from 241.0 kJ mol^{-1} for X = F to 207.4 kJ mol^{-1} for X = I. The central barriers are considerably greater than those for back-side attack, which decrease from 55.5 kJ mol^{-1} for X = Cl to 42.5 kJ mol^{-1} for X = I.

(4) Analysis of our computational data in terms of frontier orbital theory suggests that elongation of the bond between the central atom and X may be a dominant factor in decreasing the unfavorable nature of the front-side S_N2 reaction with retention of configuration in going from X = F to X = I.

(5) Ion−molecule complexes $CH_3-X\cdots X^-$ which may be pre-reaction complexes in direct collinear halophilic attack were found for X = Br and I, but not for X = F and Cl. The calculated complexation energies (ΔH_{comp}) for these halophilic complexes are considerably smaller (7.3 kJ mol^{-1} for X = Br, 19.4 kJ mol^{-1} for X = I) than those for the corresponding pre-reaction complexes for S_N2 attack at carbon (41.1 kJ mol^{-1} for X = Br, 36.0 kJ mol^{-1} for X = I).

(6) Nucleophilic substitution reactions at the halogen atom in CH_3X (X = F−I) (halophilic reactions) leading to either $CH_3^- + X_2$ or $CH_3^\bullet + X_2^{\bullet-}$ are strongly endothermic and are unlikely to compete with either back-side or front-side S_N2 reactions at the methyl carbon.

Acknowledgment. We gratefully acknowledge a generous allocation of time on the Fujitsu VP-2200 computer of the Australian National University Supercomputer Facility, the support of the Australian Research Council and of the National Science Foundation (under Grant No. CHE 94-00678 to H.B.S.), and the award (to A.P.) of an ARC Senior Research Fellowship. We also thank the Australian National University for a Visiting Fellowship (to H.B.S.) and Dr. J. J. W. McDouall for preliminary calculations.

Supporting Information Available: Table of calculated G2-(+) total energies for species involved in the $X^- + CH_3X$ identity reaction with retention of configuration (1 page). See any current masthead page for ordering and Internet access instructions.

JA9620191

(51) Stohrer, W.-D. *Chem. Ber.* **1974**, *107*, 1795.
(52) Wiberg, K. B.; McMurdie, N. *J. Am. Chem. Soc.* **1991**, *113*, 8995.
(53) Location of $[H_3C\cdots X\cdots X]^-$ transition structures linking the pre-reaction complex **3** to either set of reaction products has not been attempted in this study. The high exothermicity of the reverse halophilic reactions suggests, however, that these may be barrier-free.